Neuropsychopharmacology
At the intersection of brain, behavior, and therapeutics

Main Manuscript for

Developmental pyrethroid exposure disrupts molecular pathways for circadian rhythms and synaptic plasticity in mouse brain.

Jennifer H. Nguyen[1†], Melissa A. Curtis[1†], Ali S. Imami[1], William G. Ryan[1], Khaled Alganem[1], Kari L. Neifer[1], Charlotte N. Nawor[2], Brian P. Kistler[2], Gary W. Miller[3,4], Rammohan Shukla[1], Robert E. McCullumsmith[1], James P. Burkett[1]

[1] Department of Neurosciences, University of Toledo College of Medicine and Life Sciences, Toledo, OH 43614 (current)
[2] Department of Medicine, University of Toledo College of Medicine and Life Sciences, Toledo, OH 43614 (current)
[3] Department of Environmental Health, Emory Rollins School of Public Health, Atlanta, GA 30322
[4] Department of Environmental Health Sciences, Mailman School of Public Health, Columbia University, New York, NY 10032 (current)

[†] Equal contribution.

*Corresponding author:
James P. Burkett
3000 Arlington Ave
Block Health Sciences #185
Toledo, OH 43614
419-383-4203
james.burkett@utoledo.edu

This PDF file includes:

Main Text
Figures 1 to 3

Abstract:

Neurodevelopmental disorders (NDDs) are a category of pervasive disorders of the developing nervous system with few or no recognized biomarkers. A significant portion of the risk for NDDs, including attention deficit hyperactivity disorder (ADHD), is contributed by the environment, and exposure to pyrethroid pesticides during pregnancy has been identified as a potential risk factor for NDD in the unborn child. We recently showed that low-dose developmental exposure to the pyrethroid pesticide deltamethrin in mice causes male-biased changes to ADHD- and NDD-relevant behaviors as well as the striatal dopamine system. Here, we used a multiomics approach to determine the broadest possible set of pharmacologically relevant changes in the mouse brain caused by developmental pyrethroid exposure (DPE). Using a litter-based, split-sample design, we exposed mouse dams during pregnancy and lactation to deltamethrin (3 mg/kg or vehicle every 3 days) at a concentration well below the EPA-determined benchmark dose used for regulatory guidance. We raised male offspring to adulthood, euthanized them, and pulverized and divided whole brain samples for split-sample transcriptomics, kinomics and multiomics integration. Transcriptome analysis revealed alterations to multiple canonical clock genes, and kinome analysis revealed changes in the activity of multiple kinases involved in synaptic plasticity. Multiomics integration revealed a dysregulated protein-protein interaction network containing primary clusters for mitogen-activated protein (MAP) kinase cascades, synaptic function, and the regulation of apoptosis. These results demonstrate that DPE causes a multi-modal biophenotype in the brain relevant to ADHD and identifies new potential avenues for therapeutics.

Introduction:

Neurodevelopmental disorders (NDDs) are lifelong, incurable brain disorders with few biomarkers and few treatments[1]. The incidence of NDDs is rapidly rising, with 17% of children in the US now affected, up from 12% in 1998[2]. NDDs frequently co-occur as a cluster that includes attention deficit hyperactivity disorder (ADHD), autism, schizophrenia, intellectual disability, communication disorders, and motor and sensory disorders and share a set of common comorbidities, including epilepsy and sleep disorders[3,4]. Recently, evidence of a significant environmental component of NDD risk has been growing. Heritability estimates of autism have been falling in recent years, with large meta-analyses now estimating the environmental component at 38-48%[5]. While heritability for ADHD is high, less than 4% of the variance in ADHD diagnosis can be explained by candidate genes, suggesting that the genetic component is being inflated by gene-environment interactions[6-9]. The exploration of environmental contributors to NDD risk and their molecular mechanisms has the potential not only for future prevention but also for the discovery of new therapeutics targeting these mechanisms in children and adults.

Pyrethroid pesticides are insect-targeting neurotoxins that are the active ingredients in a wide range of products, including consumer and professional insect sprays and foggers, head lice shampoos, flea collars, and aerosol agents used for mosquito control[10]. Pyrethroid pesticides as a class are becoming some of the most widely used in the U.S. due to their low environmental impact and relative safety in adults[10]. Pyrethroid use is so widespread that 70-80% of the general US population have detectable pyrethroid metabolites in their blood, indicating an exposure within days[11,12]. Nonetheless, evidence is building that there is a risk for NDD from ambient residential pyrethroid pesticide exposure, particularly during pregnancy. Epidemiology studies have shown that women who, during pregnancy, lived in areas where pyrethroids were used were at greater risk for their unborn child to later be diagnosed with an NDD[13-15]. The level of pyrethroid metabolites in the blood of pregnant women is associated with adverse neural and mental development outcomes in the child[16]. Further, pyrethroid metabolite levels in the blood are associated with self-reported ADHD diagnosis[11,12].

To follow up on these correlational findings in humans, mouse models of pyrethroid exposure have been developed[11,17-24]. These models have established that exposure in mice to the pyrethroid deltamethrin during pregnancy and lactation at doses well below the EPA benchmark dose of 14.5 mg/kg is sufficient to cause broad male-biased changes in the brain and behavior of the resulting offspring. Male mice with developmental pyrethroid exposure (DPE) display hyperactivity, impulsivity, repetitive behaviors, diminished vocalizations, and impaired learning[11,24]. These behavioral changes are in part caused by changes in the striatal dopamine system, including elevated dopamine transporter and

dopamine D1 receptor expression, elevated striatal dopamine and dopamine metabolites, and increased peak dopamine release. Other neurological changes have also been observed from developmental and acute exposures, including alterations in levels of voltage-gated sodium channels and brain-derived neurotrophic factor (BDNF), as well as decreased neurogenesis and increased endoplasmic reticulum stress[17-20]. These findings suggest that changes in the brain may be much broader than those represented by the largely hypothesis-driven studies performed to date.

A complex biological system such as the brain functions at many biological levels simultaneously, including DNA, mRNA, proteins, and metabolites, each of which can be influenced by a disease or toxin. Any of these changes individually, or multiple multimodal changes across levels, may result in alterations in cellular function that produce a phenotype. RNA sequencing has been used to analyze the pathogenesis of many diseases and shows great potential for the identification of therapeutically significant pathways[25]. Further, kinases play a critical role in signal transduction, control most cellular functions, and are abnormally phosphorylated in a wide range of diseases, making kinome array profiling (i.e., functional proteomics) an intriguing avenue for the identification of kinases as potential druggable targets[26-31]. Using a combination of high-throughput omics analyses, we can gain a much greater insight into disease mechanisms than with a single omics dataset, allowing for a more in-depth investigation of the underlying biology of the system, potential associations, and other observed effects.

Here, we used split-sample transcriptomics and kinomics to explore, in a hypothesis-free way, the effects of developmental deltamethrin exposure as previously described[24] on the mouse brain at the level of gene transcription and protein activity. Because virtually all prior effects observed in mice were male-biased[11,24], we chose to focus on male mice. We then combined our transcriptomics and kinomics datasets using multiomics integration analyses to identify multi-modal effects. We hypothesize that indirect developmental deltamethrin exposure via the mother leads to a multi-modal biophenotype in the offspring that may be related to their NDD-relevant behavioral phenotype.

Materials and Methods:

Animals. Experimental subjects were the adult (P56+) male offspring of female C57BL6/J or C57BL6/CR mouse dams. Nulliparous female mice were socially housed in pairs on a 12/12-h light cycle and given water and high-fat breeder food ad libitum. Female pairs were then housed with a male sire until three days prior to birth, at which time they were placed in single housing. The resulting offspring were weaned at 20-22 days of age into same-sex cages and given water and standard mouse diet ad libitum. All procedures were approved by the Emory University IACUC and performed in accordance with the US Animal Welfare Act.

Study design. The design consisted of two independent groups. Dams were exposed orally to either a low dose of the pyrethroid pesticide deltamethrin (DPE group) or vehicle only (control group) every 3 days throughout pre-conception, pregnancy, and weaning as described below and previously[24]. The subjects of the experiment consisted of a single behaviorally naïve adult male offspring selected from each litter.

Experimental units. Because the exposure occurred in the dam, this study employed a litter-based design, with the dam and the litter together counting as a single experimental unit of N=1. A single behaviorally naïve adult male offspring from each litter was chosen at random for tissue collection. Therefore, the N for each analysis represents both the number of subjects and the number of dams/litters.

Sample size and elimination criteria. Dams were eliminated from the study if they did not consistently consume the pesticide when offered (as described below) or if they did not give birth to a litter containing at least two male and two female pups within 28 days of the introduction of the sire. This litter composition was needed because at least one male and one female per litter were used separately for behavioral studies[24]. A total of 40 dams were offered doses of the pesticide or vehicle (20 per group) as described below. Three dams were eliminated for incomplete consumption; two dams were eliminated for not producing a litter within 28 days; four dams were eliminated for insufficient litter size/composition; and the remaining N=31 dams produced appropriate litters for the study (control N=14, DPE N=17).

Blinding. Litters were weaned into same-sex cages, which were assigned random numbers that were used for all subsequent purposes. Control and experimental aliquots (described below) were prepared and blindly labeled as A or B. Experimenters remained blind to the identity of the treatments until after data analysis was complete.

Chemicals. Aliquots of deltamethrin (Sigma, St. Louis, MO) in corn oil (Mazola, Memphis, TN) were prepared at a concentration of 9 mg/mL by dissolving deltamethrin powder in acetone (Sigma), mixing the acetone with corn oil, evaporating the acetone from the mixture overnight in a fume hood, and storing the resulting corn oil in glass vials at -80° C. Vehicle aliquots were prepared using the same volumes of acetone and corn oil. Aliquots were thawed immediately prior to use. Dams were weighed immediately before each feeding and the appropriate amount of corn oil (1 µL/3 g body weight) was mixed with ~100 mg JIF peanut butter (J.M. Smucker, Orville, OH) to achieve a dose of 3 mg/kg.

Developmental pyrethroid exposure (DPE). Mice were developmentally exposed to the pyrethroid pesticide deltamethrin as previously described[24]. Briefly, dams were given voluntary access to peanut butter containing deltamethrin (3 mg/kg) or vehicle once every 3 days during pre-conception (2 weeks), pregnancy, and lactation. Peanut butter was given during the light cycle, and dams were allowed up to 4 hours for voluntary consumption. Dams that failed to consume 90% of the peanut butter during 90% of the feedings were eliminated from the study. Offspring were only exposed to deltamethrin indirectly through the dam. Offspring were weaned from the dam as above and received no additional treatment until adulthood.

Tissue. Adult male offspring were sacrificed by rapid decapitation and dissected, and the brains were flash-frozen using liquid nitrogen and stored at -80° C until needed. Frozen sagittal half-brain tissue samples (randomized for side) from each of the 31 subjects were pulverized and the powder aliquoted for use in split-sample multiomics.

Transcriptomics sample processing. RNA extraction was performed on N=31 homogenized half-brain tissue aliquots using the RNeasy Plus Micro Kit (QIAGEN, Germantown, MD). Tissue aliquots were homogenized in 350 µl QIAGEN Buffer RLT Plus using a Qiagen TissueLyser LT and centrifuged for 3 min at maximum speed. Supernatant was removed by pipetting and transferred to a QIAGEN gDNA Eliminator spin column placed in a 2-ml collection tube. The lysate was centrifuged for 30 s at >10,000 rpm to remove DNA contamination from the extract. The flow-through was saved, and 350 µl 70% ethanol was added and mixed well by pipetting. The entire sample was transferred to a QIAGEN RNeasy MinElute spin column placed in a 2-ml collection tube and centrifuged for 15 s at 10,000 rpm. Next, 700 µl Buffer RW1 was added to the MinElute spin column and centrifuged for 15 s at 10,000 rpm. Buffer RPE (500 µl) was added to the MinElute spin column and centrifuged for 15 s at 10,000 rpm. Finally, 500 µl 80% ethanol was added to the MinElute spin column and centrifuged for 2 min at 10,000 rpm to wash the spin column membrane. The spin column was placed into a new 2-ml collection tube and centrifuged for 5 min at full speed to dry the membrane. The spin column was added to a new 1.5-ml collection tube, with 14 µl of RNase-free water added directly to the center of the spin column membrane. RNA was eluted with 1-min centrifugation at full speed. Two aliquots of RNA extract were prepared for each sample: one for RNA concentration and purity analysis and the other to be flash frozen in a dry ice and ethanol mixture. The frozen RNA extracts were then sent overnight on dry ice (via FedEx) to the University of Michigan Advanced Genomics Core (Ann Arbor, MI) to undergo quality control, library preparation and Next Generation Sequencing. The Total RNA Library was prepared using the Illumina NovaSeq (S4) 300 cycle flow cell and reagent kit (Illumina, San Diego, CA). The high-throughput sequencing strategy included 300 cycles and a read length of paired-end 150 base pairs, with the potential to yield approximately 8-10 billion reads from our 31 subject samples.

An aliquot of extracted RNA for each subject was assayed using a NanoDrop One (Thermo Scientific, Waltham, MA) to determine sample RNA concentration and purity. A 260/280 ratio of 2 indicates pure RNA with no protein contamination. All samples used in the study passed the RNA quality check. The quality of the RNA was also measured using Agilent Bioanalyzer. All samples had an RNA integrity number (RIN) > 7, indicating high-quality RNA.

Transcriptomics quality control. The University of Michigan Advanced Genomics Core sent the results of the Total RNA Library in the form of paired end FASTQ files containing sample sequences, via Globus, for further processing through the Ohio Supercomputer Center. With the Total RNA method, 959,825,599 reads were obtained from our samples. The sample sequences underwent quality control analysis using the MultiQC tool. All samples showed high quality except for overrepresented adapter sequences near the end of each sequence, which were removed using the Trimmomatic version 0.36[32]. All samples showed high quality after trimming. After assuring quality, we used Hisat2 and Samtools to align the

FASTQ files to the mouse reference genome GRCm38, convert files (from sam to bam), map and count the reads, and remove batch effects using surrogate variable analysis[33,34].

Differential gene expression analysis. Differential gene expression analysis was performed on the count data matrix using DEseq2, chosen since the normalization median of ratios method implemented is based on the hypothesis that most genes are not differentially expressed[35]. DEseq2 also performs independent filtering and per-gene outlier detection using Cook's distance, making it the favored method[36].

Hierarchical clustering analysis. We performed hierarchical clustering analysis using the top 100 differentially expressed genes ($p<0.05$) from the differential gene expression dataset and generated a heatmap to visualize differences between the two groups. To further investigate potential differences between the groups, we extracted the number of differentially expressed genes based on their corresponding p-values. Due to the confirmed lack of biological differences, we continued our analysis using genes that were considered significant by using the cutoff of an adjusted p-value<0.05.

Transcription factor and kinase enrichment analysis. The web tools CHEA3[37] and KEA3[38] were used to perform transcription factor enrichment analysis and kinase enrichment analysis, respectively, using the top 100 differentially expressed genes from the DEseq2 analysis. CHEA3 and KEA3 compute enrichment scores for transcription factors and kinases likely to regulate the expression of the differentially expressed genes to predict their involvement in the observed changes in gene expression.

Kinomics sample processing. One of the five homogenized sample aliquots was used to measure kinase activity. Lysis buffer was prepared using a 1:100 dilution of M-PER Mammalian Extraction Buffer (Thermo Scientific) to EDTA-free Halt Protease Inhibitor Cocktail (Thermo Scientific) and stored on ice. The sample aliquot was then lysed in the appropriate amount of lysis buffer (3x sample volume) and incubated for 30 min on ice. The lysate was then centrifuged for 15 min at 16,000 g in a pre-cooled centrifuge in a 4°C refrigerator. The supernatant was then extracted and separated into 3 aliquots of equal volume (~15 µl), as freeze thaw cycles can result in loss of kinase activity. One aliquot was set aside for immediate use for protein quantification. The other two aliquots were immediately flash frozen in a dry ice and ethanol mixture and then stored at -80°C until use by the core.

Protein quantification was performed on each sample via a BCA Protein Assay with appropriate standards and reagents. We made standards using BSA stock solution (2 mg/ml), hypertonic buffer, and H_2O. We added 30 µl of each standard to the designated well in duplicates (n=2) and 2 µl of sample to designated wells with 28 µl of H_2O in triplicates (n=3). The blank in our assay used BCA buffer +30 µl of H_2O only. We made a 50:1 mixture of Reagent A to Reagent B, 250 µl which was then added to each well on the 96-well count plate. The plate sat and incubated at room temperature for 30 min. The plate was read at 562 nm with the appropriate plate measurements on SoftMax Pro software. The results were collected and transferred to an Excel document for analysis. Concentrations were determined utilizing the standard curve and level of absorption generated from each sample and used to make the appropriate dilutions prior to transferring samples to the Core Facility.

On the day of processing, the University of Toledo Kinome Array Core Facility performed high-throughput kinase activity profiling on the sample lysates, using the Pamstation12 instrument and the PamChip assay (PamGene, 's-Hertogenbosch, The Netherlands). The Pamstation12 can be loaded with either a serine/threonine or phosphotyrosine microarray chip, accommodating 3 chips per run. Each chip contains 4 wells, where 4 samples can be loaded. The chips function as microarrays, representing 144 (STK chip) or 196 (PTK chip) reporter peptides that can be phosphorylated by various kinases. Each of the 4 wells in the chip contain well-validated target peptides. Protein kinases is the sample may then phosphorylate target peptides when loaded in the presence of ATP. The Pamstation12 instrument then measures the phosphorylation of these reporter peptides in real time by detecting and imaging fluorescently labeled antibodies at different exposure times and provides the output of each sample's kinase activity [39]. The PamChip arrays were the optimal array for our experiments because they are designed to allow peptide substrates to be deposited at higher concentrations than conventional arrays, thus increasing sensitivity.

The serine threonine kinase (STK) chip can be loaded with a maximum of 2.2 µg of protein per individual array well. The phosphotyrosine kinase (PTK) chip can be loaded with a maximum of 10 µg of protein per individual array well. To meet the appropriate total protein concentrations, the previously

frozen extracts were thawed on ice and diluted using ice-cold M-PER buffer concentration (STK total protein = 2.2 µg in 11 µl required volume; PTK total protein = 11 µg in 11 µl required volume). The diluted first-thaw lysate material was then added to 10 µl of MPER buffer and an additional 1 µl of Inhibitor Cocktail, for a total 11 µl of lysate of extract for each sample[39]. These extracts were then taken on ice to the University of Toledo Kinome Array Core to be run on the PamGene12 Station. All 31 samples were run on both the STK and PTK chips. Six runs were performed in total, three for STK and the other three for PTK activity profiling.

Kinomics data analysis. The BioNavigator software tool was used to preprocess the kinome data, perform image analysis, interpret output measurements, and to visualize, store, and share the results for each of our six runs. The Kinome Random Sampling Analyzer (KRSA) is a validated R package for kinome array analysis and was implemented to identify differential phosphorylation and to predict upstream kinase activity and network modeling[40]. This tool allows for a better understanding of kinase interactions and global changes that occur between two states. The output of KRSA is a Z-score value. This value represents the difference between the observed value of a kinase from what you would expect in a random sample. A z-score threshold of 2 was used to determine which kinases were “hits” for downstream analyses.

Network-based multiomics integration of transcriptome and kinome. We used the Kinograte R package[41], which implements an optimized version of the PCSF algorithm[42], to generate an integrated multiomic protein-protein interaction (PPI) network consisting of transcriptomic “hits” ($p < 0.05$) and kinase “hits” ($|Z| > 1.5$) with node prizes assigned by percentile rank of respective $\log_2$ fold change (Log2FC) or Z score and edge costs assigned by inverse STRING-DB3 interaction confidence. The PPI network nodes were ranked by an average of their node prize and eigencentrality, and these node rankings were used as input for gene-set enrichment analysis using the FGSEA R package[43] with the Gene Ontology database[44]. Dysregulated pathways from FGSEA (FDR < 0.05) were then functionally clustered and visualized using PAVER[45], a meta-clustering method for pathways.

Results:

Transcriptome. We performed transcriptomic analysis to compare brain-wide RNA expression in male DPE mice to the expression in vehicle controls. Differential gene expression analysis identified exactly two genes that differed in their brain-wide expression levels in DPE mice, both of which are canonical clock genes: period circadian regulator 2 (PER2, Log2FC = -0.35, p = 0.014) and circadian-associated repressor of transcription (CIART, Log2FC = -0.42, p = 0.042) (Figure 1, Supplementary File 1A). Hierarchical clustering analysis showed that transcription changes as a whole were not clustered by treatment group (Figure S1). Transcription factor enrichment analysis predicted a set of transcription factors upstream of changes in gene transcription, including three putative immediate early genes (FOSB, CSRNP1, CSRNP3) and two transcription factors related to neurogenesis (CXXC4, SOX4), among others (Supplementary File 1B). Kinase enrichment analysis predicted kinases upstream of changes in transcription that were related to circadian rhythms (CSNK1D, CSNK1E, PAK1) and mitogen-activated protein (MAP) kinase/mammalian target of rapamycin (mTOR) cascades (MAPK1/ERK2, MAPK3/ERK1, MAPK14/p38α, SGK1) (Supplementary File 1C).

Kinome. We performed kinase activity profiling to detect brain-wide changes in kinase activity in DPE mice. KRSA analysis of differential phosphorylation patterns identified seven kinases with differential activity in DPE mice ($Z > 1.5$), all of which have primary roles in synaptic plasticity (PKCH, PAKB, PKN, MLCK, ERK, BRSK, and PIM), and one of which is a prominent MAP kinase (ERK) (Figure 2, Figure S2).

*Multi-omics Integration***.** To detect multi-modal changes in molecular pathways, we performed a multi-omics integration of the transcriptome and kinome datasets. Multimodal gene set enrichment analysis returned 521 significantly altered gene sets that clustered into 13 pathways, including MAP kinase cascades, regulation of apoptosis, and synaptic function, among others (Figure 3A-C, Supplementary File 1D). This analysis generated a protein-protein interaction (PPI) network with AKT and MAPK3/ERK1 as major hubs (Figure 3D, Figure S2, Supplementary File 1E, Supplementary File 2).

Discussion

We have developed a mouse model of DPE, which is a risk factor in humans for autism and ADHD. Using a split-sample multi-omics approach, we detected a multi-modal biophenotype in the brains of mice developmentally exposed to the pyrethroid pesticide deltamethrin. The brain-wide expression level of genes related to circadian rhythms was altered by developmental exposure. There were also brain-wide changes in the activity level of a wide range of kinases related to synaptic plasticity and dendritic spines. Statistical integration of transcriptome and kinome data revealed disruptions in multi-modal molecular pathways clustered around growth/apoptosis, the MAP kinase cascades, and synaptic function. Overall, we have identified a range of specific targets that may be associated with the neurodevelopmental disorder-related behavioral phenotypes observed in these developmentally exposed mice, including hyperactivity, repetitive behaviors, decreased vocalizations, and cognitive deficits[24].

Disruptions in synaptic plasticity and dendritic spines have been implicated in the etiology of autism, ADHD, and neurodevelopmental disorders in general[46-48], and these disruptions are some of the most commonly replicated observations in mouse models of autism risk[49,50]. All seven kinases with differential kinase activity in DPE mice have roles in synaptic plasticity, and synapse function was identified as a significant cluster in the multi-omics network. Protein kinase C (PKC) has a long-established role in long-term potentiation and NMDA regulation[51-53]. Protein kinase N, a member of the PKC superfamily, directly interacts with AKT (the primary hub of our multi-omics network) and may have a specific role in synapse maturation[54,55]. The ERK/MAP kinase cascade regulates transcriptional events related to synaptic plasticity[56]. PAKB (a differentially active kinase) and PAK1 (identified by transcriptomic kinase enrichment analysis) are both PAK family kinases that play roles in long-term potentiation and dendritic morphology and can regulate MAP kinase[57-59]. MLCK, BRSK, and PIM also play roles in various aspects of pre- and post-synaptic signaling and synapse formation[60-62]. Overall, this collection of observations suggests that disruptions in synaptic function and/or dendritic spines are potential biophenotypes in DPE mice that may underlie the learning deficits observed in this model[24].

The MAP kinase and mTOR signaling pathways are known to interact to co-regulate various cellular processes related to cell growth and apoptosis[63,64] and both have been linked to neurodevelopmental disorders including autism and epilepsy[59,65,66]. In addition to their canonical roles in cell growth and differentiation, MAP kinases interact with the mTOR signaling pathway to facilitate dendritic growth and spine formation[63,67]. The kinase activity of the MAP kinase ERK was altered in DPE mice, and a transcriptional network of transcription factor-kinase pathways altered in DPE mice predicted changes in MAPK1 (ERK2), MAPK3 (ERK1), MAPK14 (p38α), and the mTOR-related kinase SGK1. AKT, a central component of the mTOR pathway, was also the predicted hub of the multi-omics protein-protein interaction network. Among the multi-modal gene set clusters distinguishing DPE mouse brains from controls, the most enriched cluster was for the MAP kinase cascade, while the largest cluster was for regulation of apoptotic processes. This cluster of gene sets regulating apoptotic processes may be due to a primary effect of DPE on adult neurogenesis, as has been seen in adult mice[18], or may be driven by the dual role of MAP kinase and mTOR pathways in both inhibiting apoptosis and promoting dendritic spine growth. Finally, the transcriptional network of transcription factor-kinase pathways altered in DPE mice predicted roles for the transcription factors CSRNP1, CSRNP3, and FOSB (among others), all of which are putative or proposed immediate early genes that correlate with neuronal activity. Overall, these results bolster the hypothesis that pathways regulating spines and synapses are dysfunctional in DPE mice.

Disrupted sleep-wake patterns, sleep-onset difficulty, and altered diurnal melatonin patterns have been reported in autism and ADHD[68-73]. DPE mice showed transcriptional changes in two canonical clock genes regulating circadian rhythms, PER2 and CIART/CHRONO, which were sufficient to survive genome-wide correction at the whole-brain level. Of note, DBP, the third most differentially expressed gene which did not survive genome-wide corrections, is a transcription factor related to circadian regulation. A transcriptional network of transcription factor-kinase pathways altered in DPE mice also predicted roles for the circadian rhythm-related transcription factors CSRNP1 and FOSB, and the kinases casein kinase 1D, casein kinase 1E, PAK1, and PKC eta. The suprachiasmatic nucleus traditionally controls the “master clock” for circadian rhythms in the brain, and yet this region is vanishingly small and unlikely to be detected in whole brain homogenate[74]. Therefore, these changes in clock-related gene transcription are likely to be pervasively represented in local clocks throughout the brain and may indicate either a primary effect of DPE on local clock function, or any number of deficiencies in the function of the

suprachiasmatic nucleus that are then carried forward. While circadian rhythms were not assessed behaviorally in DPE mice, these mice did show persistent hyperactivity[24]. Assessment of circadian rhythms in this model is an important future direction.

A critical strength of this study was the use of an integrative multi-omics approach. Our primary goal was to identify, in the broadest possible sense, the molecular pathways altered by DPE. To accomplish this goal, we used a split-sample approach to maximize the inter-relationship between transcriptome and kinome data. We then employed statistical methods to integrate across data sets in order to examine the emergent multimodal biophenotype across multiple levels of evidence. This holistic, integrative approach to combining multi-omics data highlights the interrelationships of the involved biomolecules and their functions and avoids bias in interpreting parallel data sets[75,76].

Our gene expression and kinase activity data were generated from samples of homogenized whole brain tissue from mice. Because DPE is a whole-body manipulation, we selected whole-brain tissue as the most appropriate level for initial investigation and did not focus on a specific brain region or cell type. This represents both a significant limitation and a critical strength: any pathways that are disrupted brain-wide in dominant cell types are likely to be good targets for pharmaceutical intervention, while pathways that are not disrupted brain-wide in dominant cell types are unlikely to be represented in our dataset.

The use of a single exposure dose of deltamethrin is a key limitation for this study. Our exposure dose was based on prior studies using this model in which 3 mg/kg developmental exposure was sufficient to cause a broad behavioral and neurological phenotype relevant to neurodevelopmental disorders[11,24]. This dose is well below the lower confidence limit of the benchmark dose (LBMD, 10.1 mg/kg) used for regulatory guidance[10]. Nonetheless, a critical next step would be to carefully study the exposure-dependent accumulation of deltamethrin and its metabolites in a variety of tissues and to examine in parallel the dose-dependent effects of exposure on the brain and behavior.

Pesticides are widely used around the world, making pesticide exposures during development and adulthood common. Pyrethroid pesticides, while widely considered safe for adults, have been linked to autism and neurodevelopmental disorders in humans and cause related behavioral changes in mice. Here, we show that DPE in mice causes broad changes in molecular pathways in the brain for circadian rhythms and synaptic plasticity. These findings may suggest potential future avenues for medical treatments for these disorders by targeting these molecular pathways.

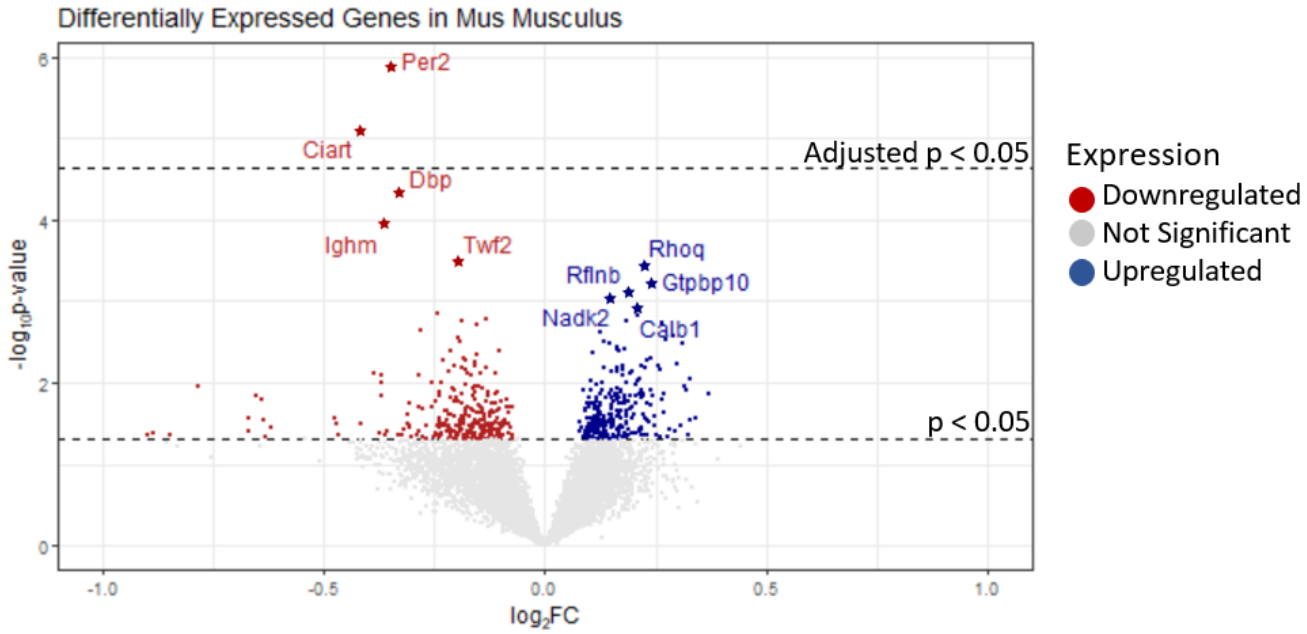

Gene	Log_2 Fold Change	Adjusted p
Per2	-0.35	0.014
Ciart	-0.42	0.042

Figure 1. Volcano plot of differential gene expression analysis comparing whole-brain tissue from control and DPE mice, plotted as a function of the $\log_2$ fold change in gene expression and the inverse $\log_{10}$ of the p-value. Dashed lines demarcate raw and adjusted p-values below 0.05.

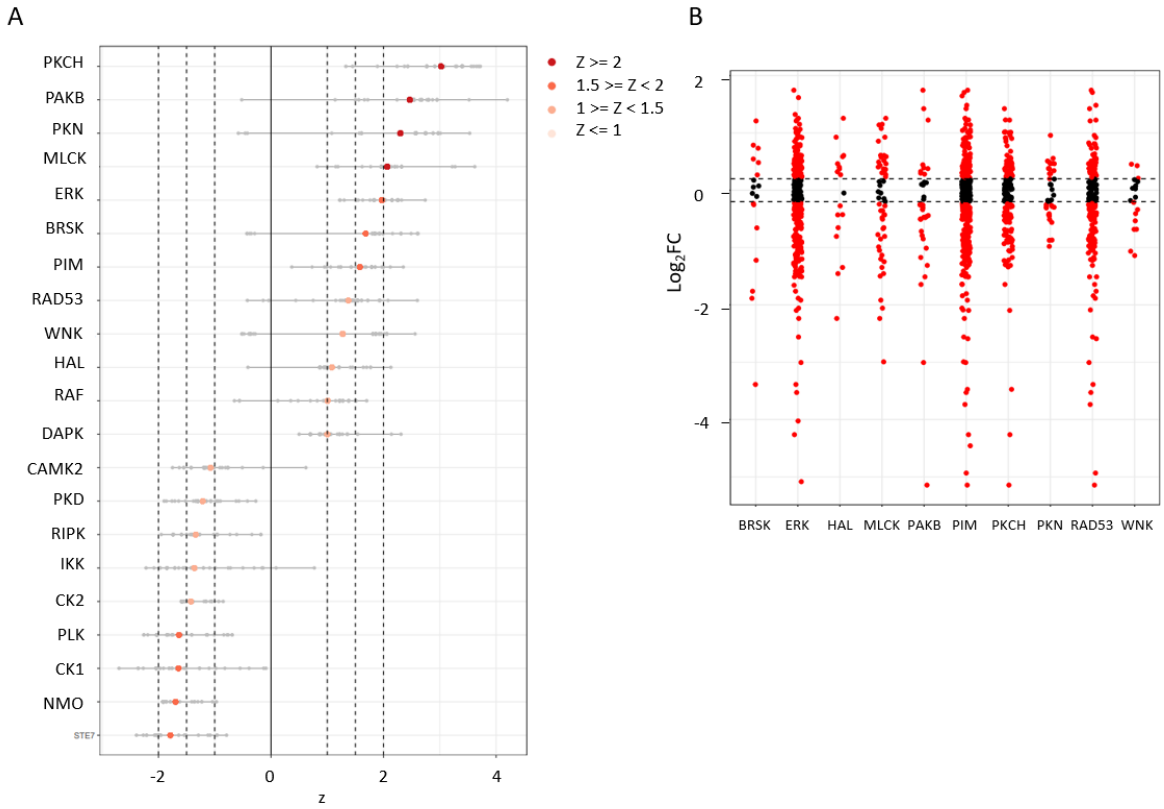

Figure 2. Identification of differentially active tyrosine kinase families identified in whole-brain tissue of DPE mice. (A) Waterfall plot of serine-threonine kinases predicted to be differentially active as a result of differentially phosphorylated peptide substrates on the kinome array chips. (B) Fold-change of phosphorylated substrates related to the top 10 differentially active kinases, showing that most differentially active kinases have reduced activity in DPE mice.

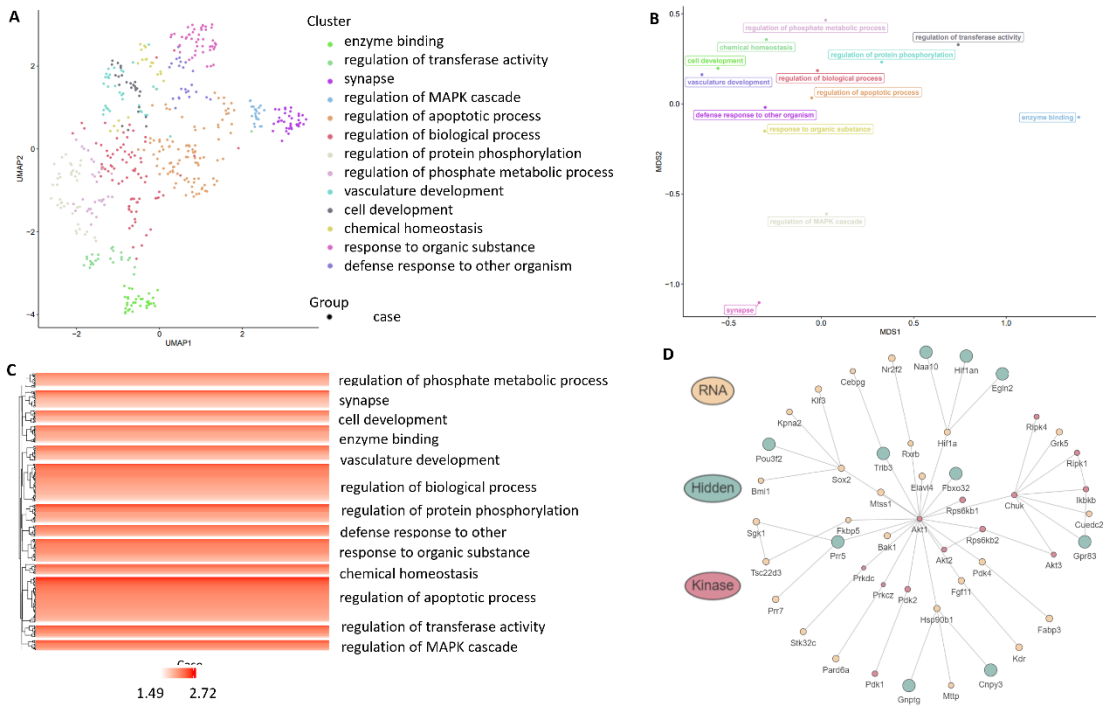

Figure 3. Identification of multi-modal molecular pathways altered in DPE mice using integrative multi-omics. (A) UMAP principal components analysis of dysregulated molecular pathways identified 13 distinct gene set clusters. (B) MDS principal components analysis showing the interval scale distance in component space between the clusters. (C) Pathway cluster heatmap showing, from least to most dense, the normalized enrichment scores of the identified hierarchical pathway clusters. (D) The 2nd-degree protein-protein interaction network for the primary PPI network hub protein, AKT1.

Acknowledgements:

We would like to thank S. Daniel of In Scripto, LLC for comments on this manuscript. My family did not help in any way with this manuscript and were quite distracting. I would like to acknowledge Meggin, Kyle, Calvin, and Becky.

Author Contributions:

JPB and GWM designed the exposure study, and JPB and REM designed the multiomics strategy and experiments. All samples were collected in the lab of GWM by JPB and transferred to the lab of JPB. MAC processed all samples, distributed them to the core facilities, and coordinated the initial analysis of all data. JHN, ASI, KA, and WGR participated in the final analysis of all data and assembly of figures under the guidance of JPB, RS, and REM. JPB, MAC, and JHN interpreted all results. CNN and BPK performed background research and assisted in manuscript preparation. KLN provided experimental, administrative, and managerial support. All authors participated in writing the manuscript and approved the final version.

Funding:

This research was supported in part by funding from the NIH to JPB (NIEHS: R00ES027869) and to GWM (NIEHS: R01ES023839). This research was also supported by an award to JPB from the deArce-Koch Memorial Endowment Fund. Stipend support was provided to CNN and BPK by the UToledo Medical Student Research Program.

Competing Interest Statement:

The authors declare no competing interests.

Data Availability Statement:

All sequencing data are available on NCBI GEO (GSE241185). All raw kinome array data are available on Zenodo (DOI: 10.5281/zenodo.8283637). All code used to analyze the data is on GitHub repository v1.0 (https://github.com/JamesBurkett7/DPE-disrupts-molecular-pathways-manuscript.git). All metadata, including comprehensive statistical results (differential gene expression, CHEA, KEA, FGSEA, Kinograte) and protein-protein interaction networks, are available in the supplementary materials.

Bibliography:

1 Silverman, J. L. *et al.* Reconsidering animal models used to study autism spectrum disorder: Current state and optimizing future. *Genes Brain Behav* **21**, e12803 (2022). https://doi.org:10.1111/gbb.12803

2 Cogswell, M. E. *et al.* Health Needs and Use of Services Among Children with Developmental Disabilities - United States, 2014-2018. *MMWR Morb Mortal Wkly Rep* **71**, 453-458 (2022). https://doi.org:10.15585/mmwr.mm7112a3

3 Homberg, J. R. *et al.* Understanding autism and other neurodevelopmental disorders through experimental translational neurobehavioral models. *Neurosci Biobehav Rev* **65**, 292-312 (2016). https://doi.org:10.1016/j.neubiorev.2016.03.013

4 Aschner, M. & Costa, L. G. *Environmental factors in neurodevelopmental and neurodegenerative disorders*. (Elsevier/Academic Press, 2015).

5 Huguet, G., Ey, E. & Bourgeron, T. The genetic landscapes of autism spectrum disorders. *Annual review of genomics and human genetics* **14**, 191-213 (2013).

6 Smith, A. K., Mick, E. & Faraone, S. V. Advances in genetic studies of attention-deficit/hyperactivity disorder. *Curr Psychiatry Rep* **11**, 143-148 (2009). https://doi.org:10.1007/s11920-009-0022-0

7 Matthews, M., Nigg, J. T. & Fair, D. A. Attention deficit hyperactivity disorder. *Curr Top Behav Neurosci* **16**, 235-266 (2014). https://doi.org:10.1007/7854_2013_249

8 Kim, J. H. *et al.* Environmental risk factors, protective factors, and peripheral biomarkers for ADHD: an umbrella review. *Lancet Psychiatry* **7**, 955-970 (2020). https://doi.org:10.1016/S2215-0366(20)30312-6

9 Froehlich, T. E. *et al.* Update on environmental risk factors for attention-deficit/hyperactivity disorder. *Curr Psychiatry Rep* **13**, 333-344 (2011). https://doi.org:10.1007/s11920-011-0221-3

10 *Pyrethrins/pyrethroid cumulative risk assessment* (U.S Environmental Protection Agency, Washington DC, 2011).

11 Richardson, J. R. *et al.* Developmental pesticide exposure reproduces features of attention deficit hyperactivity disorder. *The FASEB Journal* **29**, 1960-1972 (2015).

12 Wagner-Schuman, M. *et al.* Association of pyrethroid pesticide exposure with attention-deficit/hyperactivity disorder in a nationally representative sample of U.S. children. *Environ Health* **14**, 44 (2015). https://doi.org:10.1186/s12940-015-0030-y

13 Shelton, J. F. *et al.* Neurodevelopmental disorders and prenatal residential proximity to agricultural pesticides: the CHARGE study. *Environmental health perspectives* **122**, 1103-1109 (2014).

14 Hicks, S. D., Wang, M., Fry, K., Doraiswamy, V. & Wohlford, E. M. Neurodevelopmental Delay Diagnosis Rates Are Increased in a Region with Aerial Pesticide Application. *Front Pediatr* **5**, 116 (2017). https://doi.org:10.3389/fped.2017.00116

15 von Ehrenstein, O. S. *et al.* Prenatal and infant exposure to ambient pesticides and autism spectrum disorder in children: population based case-control study. *BMJ* **364**, l962 (2019). https://doi.org:10.1136/bmj.l962

16 Xue, Z. *et al.* Effect of synthetic pyrethroid pesticide exposure during pregnancy on the growth and development of infants. *Asia Pac J Public Health* **25**, 72S-79S (2013). https://doi.org:10.1177/1010539513496267

17 Magby, J. P. & Richardson, J. R. Developmental pyrethroid exposure causes long-term decreases of neuronal sodium channel expression. *Neurotoxicology* **60**, 274-279 (2017). https://doi.org:10.1016/j.neuro.2016.04.002

18 Hossain, M. M., Belkadi, A., Al-Haddad, S. & Richardson, J. R. Deltamethrin Exposure Inhibits Adult Hippocampal Neurogenesis and Causes Deficits in Learning and Memory in Mice. *Toxicol Sci* **178**, 347-357 (2020). https://doi.org:10.1093/toxsci/kfaa144
19 Hossain, M. M., Sivaram, G. & Richardson, J. R. Regional Susceptibility to ER Stress and Protection by Salubrinal Following a Single Exposure to Deltamethrin. *Toxicol Sci* **167**, 249-257 (2019). https://doi.org:10.1093/toxsci/kfy238
20 Hossain, M. M., DiCicco-Bloom, E. & Richardson, J. R. Hippocampal ER stress and learning deficits following repeated pyrethroid exposure. *Toxicol Sci* **143**, 220-228 (2015). https://doi.org:10.1093/toxsci/kfu226
21 Armstrong, L. E. *et al.* Effects of developmental deltamethrin exposure on white adipose tissue gene expression. *J Biochem Mol Toxicol* **27**, 165-171 (2013). https://doi.org:10.1002/jbt.21477
22 Vester, A. I. *et al.* Combined neurodevelopmental exposure to deltamethrin and corticosterone is associated with Nr3c1 hypermethylation in the midbrain of male mice. *Neurotoxicol Teratol* **80**, 106887 (2020). https://doi.org:10.1016/j.ntt.2020.106887
23 Vester, A. I., Chen, M., Marsit, C. J. & Caudle, W. M. A Neurodevelopmental Model of Combined Pyrethroid and Chronic Stress Exposure. *Toxics* **7** (2019). https://doi.org:10.3390/toxics7020024
24 Curtis, M. A. *et al.* Developmental pyrethroid exposure causes a neurodevelopmental disorder phenotype in mice. *PNAS Nexus* (In press).
25 Shukla, R. *et al.* Signature-based approaches for informed drug repurposing: targeting CNS disorders. *Neuropsychopharmacology* **46**, 116-130 (2021). https://doi.org:10.1038/s41386-020-0752-6
26 Gomase, V. S. & Tagore, S. Kinomics. *Current drug metabolism* **9**, 255-258 (2008).
27 McGuire, J. L. *et al.* Altered serine/threonine kinase activity in schizophrenia. *Brain Res* **1568**, 42-54 (2014). https://doi.org:10.1016/j.brainres.2014.04.029
28 Dorsett, C. R. *et al.* Traumatic Brain Injury Induces Alterations in Cortical Glutamate Uptake without a Reduction in Glutamate Transporter-1 Protein Expression. *J Neurotrauma* **34**, 220-234 (2017). https://doi.org:10.1089/neu.2015.4372
29 Creeden, J. F. *et al.* Kinome Array Profiling of Patient-Derived Pancreatic Ductal Adenocarcinoma Identifies Differentially Active Protein Tyrosine Kinases. *Int J Mol Sci* **21** (2020). https://doi.org:10.3390/ijms21228679
30 Alganem, K. *et al.* The active kinome: The modern view of how active protein kinase networks fit in biological research. *Curr Opin Pharmacol* **62**, 117-129 (2022). https://doi.org:10.1016/j.coph.2021.11.007
31 Creeden, J. F. *et al.* Hepatic kinome atlas: An in-depth identification of kinase pathways in liver fibrosis of humans and rodents. *Hepatology* **76**, 1376-1388 (2022). https://doi.org:10.1002/hep.32467
32 Bolger, A. M., Lohse, M. & Usadel, B. Trimmomatic: a flexible trimmer for Illumina sequence data. *Bioinformatics* **30**, 2114-2120 (2014). https://doi.org:10.1093/bioinformatics/btu170
33 Kim, D., Paggi, J. M., Park, C., Bennett, C. & Salzberg, S. L. Graph-based genome alignment and genotyping with HISAT2 and HISAT-genotype. *Nat Biotechnol* **37**, 907-915 (2019). https://doi.org:10.1038/s41587-019-0201-4
34 Li, H. *et al.* The Sequence Alignment/Map format and SAMtools. *Bioinformatics* **25**, 2078-2079 (2009). https://doi.org:10.1093/bioinformatics/btp352
35 Love, M. I., Huber, W. & Anders, S. Moderated estimation of fold change and dispersion for RNA-seq data with DESeq2. *Genome Biol* **15**, 550 (2014). https://doi.org:10.1186/s13059-014-0550-8
36 Zhang, Z. H. *et al.* A comparative study of techniques for differential expression analysis on RNA-Seq data. *PloS one* **9**, e103207 (2014).

37 Keenan, A. B. *et al.* ChEA3: transcription factor enrichment analysis by orthogonal omics integration. *Nucleic Acids Res* **47**, W212-W224 (2019). https://doi.org:10.1093/nar/gkz446
38 Kuleshov, M. V. *et al.* KEA3: improved kinase enrichment analysis via data integration. *Nucleic Acids Res* **49**, W304-W316 (2021). https://doi.org:10.1093/nar/gkab359
39 Hilhorst, R. *et al.* in *Gene Regulation* 259-271 (Springer, 2013).
40 DePasquale, E. A. *et al.* KRSA: Network-based Prediction of Differential Kinase Activity from Kinome Array Data. *BioRxiv* (2020).
41 Alganem, K. *Network-Based Integration of Multi-Omics Datasets*, The University of Toledo, (2022).
42 Akhmedov, M. *et al.* PCSF: An R-package for network-based interpretation of high-throughput data. *PLoS Comput Biol* **13**, e1005694 (2017). https://doi.org:10.1371/journal.pcbi.1005694
43 Gennady, K. *et al.* Fast gene set enrichment analysis. *bioRxiv*, 060012 (2021). https://doi.org:10.1101/060012
44 Ashburner, M. *et al.* Gene ontology: tool for the unification of biology. The Gene Ontology Consortium. *Nat Genet* **25**, 25-29 (2000). https://doi.org:10.1038/75556
45 Ryan, W. *willgryan/PAVER: Pre-release to generate DOI (pre-release)*, 2023).
46 Lesch, K. P. *et al.* Molecular genetics of adult ADHD: converging evidence from genome-wide association and extended pedigree linkage studies. *J Neural Transm (Vienna)* **115**, 1573-1585 (2008). https://doi.org:10.1007/s00702-008-0119-3
47 Bourgeron, T. From the genetic architecture to synaptic plasticity in autism spectrum disorder. *Nat Rev Neurosci* **16**, 551-563 (2015). https://doi.org:10.1038/nrn3992
48 Phillips, M. & Pozzo-Miller, L. Dendritic spine dysgenesis in autism related disorders. *Neurosci Lett* **601**, 30-40 (2015). https://doi.org:10.1016/j.neulet.2015.01.011
49 Martinez-Cerdeno, V. Dendrite and spine modifications in autism and related neurodevelopmental disorders in patients and animal models. *Dev Neurobiol* **77**, 393-404 (2017). https://doi.org:10.1002/dneu.22417
50 Kazdoba, T. M., Leach, P. T. & Crawley, J. N. Behavioral phenotypes of genetic mouse models of autism. *Genes Brain Behav* **15**, 7-26 (2016). https://doi.org:10.1111/gbb.12256
51 Tanaka, C. & Nishizuka, Y. The protein kinase C family for neuronal signaling. *Annu Rev Neurosci* **17**, 551-567 (1994). https://doi.org:10.1146/annurev.ne.17.030194.003003
52 Lan, J. Y. *et al.* Protein kinase C modulates NMDA receptor trafficking and gating. *Nat Neurosci* **4**, 382-390 (2001). https://doi.org:10.1038/86028
53 Rosse, C. *et al.* PKC and the control of localized signal dynamics. *Nat Rev Mol Cell Biol* **11**, 103-112 (2010). https://doi.org:10.1038/nrm2847
54 Yasuda, H. *et al.* PKN1 promotes synapse maturation by inhibiting mGluR-dependent silencing through neuronal glutamate transporter activation. *Commun Biol* **3**, 710 (2020). https://doi.org:10.1038/s42003-020-01435-w
55 Safari, M. S., Obexer, D., Baier-Bitterlich, G. & Zur Nedden, S. PKN1 Is a Novel Regulator of Hippocampal GluA1 Levels. *Front Synaptic Neurosci* **13**, 640495 (2021). https://doi.org:10.3389/fnsyn.2021.640495
56 Thomas, G. M. & Huganir, R. L. MAPK cascade signalling and synaptic plasticity. *Nat Rev Neurosci* **5**, 173-183 (2004). https://doi.org:10.1038/nrn1346
57 Asrar, S. *et al.* Regulation of hippocampal long-term potentiation by p21-activated protein kinase 1 (PAK1). *Neuropharmacology* **56**, 73-80 (2009). https://doi.org:10.1016/j.neuropharm.2008.06.055
58 Zhao, Z. S. & Manser, E. PAK family kinases: Physiological roles and regulation. *Cell Logist* **2**, 59-68 (2012). https://doi.org:10.4161/cl.21912

59 Nussinov, R. *et al.* Neurodevelopmental disorders, like cancer, are connected to impaired chromatin remodelers, PI3K/mTOR, and PAK1-regulated MAPK. *Biophys Rev* **15**, 163-181 (2023). https://doi.org:10.1007/s12551-023-01054-9
60 Inoue, E. *et al.* SAD: a presynaptic kinase associated with synaptic vesicles and the active zone cytomatrix that regulates neurotransmitter release. *Neuron* **50**, 261-275 (2006). https://doi.org:10.1016/j.neuron.2006.03.018
61 Srinivasan, G., Kim, J. H. & von Gersdorff, H. The pool of fast releasing vesicles is augmented by myosin light chain kinase inhibition at the calyx of Held synapse. *J Neurophysiol* **99**, 1810-1824 (2008). https://doi.org:10.1152/jn.00949.2007
62 Konietzko, U. *et al.* Pim kinase expression is induced by LTP stimulation and required for the consolidation of enduring LTP. *EMBO J* **18**, 3359-3369 (1999). https://doi.org:10.1093/emboj/18.12.3359
63 Zhang, W. & Liu, H. T. MAPK signal pathways in the regulation of cell proliferation in mammalian cells. *Cell Res* **12**, 9-18 (2002). https://doi.org:10.1038/sj.cr.7290105
64 Lipton, J. O. & Sahin, M. The neurology of mTOR. *Neuron* **84**, 275-291 (2014). https://doi.org:10.1016/j.neuron.2014.09.034
65 Rosina, E. *et al.* Disruption of mTOR and MAPK pathways correlates with severity in idiopathic autism. *Transl Psychiatry* **9**, 50 (2019). https://doi.org:10.1038/s41398-018-0335-z
66 Vithayathil, J., Pucilowska, J. & Landreth, G. E. ERK/MAPK signaling and autism spectrum disorders. *Prog Brain Res* **241**, 63-112 (2018). https://doi.org:10.1016/bs.pbr.2018.09.008
67 Kumar, V., Zhang, M. X., Swank, M. W., Kunz, J. & Wu, G. Y. Regulation of dendritic morphogenesis by Ras-PI3K-Akt-mTOR and Ras-MAPK signaling pathways. *J Neurosci* **25**, 11288-11299 (2005). https://doi.org:10.1523/JNEUROSCI.2284-05.2005
68 Van der Heijden, K. B., Smits, M. G., Van Someren, E. J. & Gunning, W. B. Idiopathic chronic sleep onset insomnia in attention-deficit/hyperactivity disorder: a circadian rhythm sleep disorder. *Chronobiol Int* **22**, 559-570 (2005). https://doi.org:10.1081/CBI-200062410
69 Cortese, S., Faraone, S. V., Konofal, E. & Lecendreux, M. Sleep in children with attention-deficit/hyperactivity disorder: meta-analysis of subjective and objective studies. *J Am Acad Child Adolesc Psychiatry* **48**, 894-908 (2009). https://doi.org:10.1097/CHI.0b013e3181ac09c9
70 Konofal, E., Lecendreux, M. & Cortese, S. Sleep and ADHD. *Sleep Med* **11**, 652-658 (2010). https://doi.org:10.1016/j.sleep.2010.02.012
71 Richdale, A. L. & Prior, M. R. The sleep/wake rhythm in children with autism. *Eur Child Adolesc Psychiatry* **4**, 175-186 (1995). https://doi.org:10.1007/BF01980456
72 Cortese, S., Wang, F., Angriman, M., Masi, G. & Bruni, O. Sleep Disorders in Children and Adolescents with Autism Spectrum Disorder: Diagnosis, Epidemiology, and Management. *CNS Drugs* **34**, 415-423 (2020). https://doi.org:10.1007/s40263-020-00710-y
73 Xue, M., Brimacombe, M., Chaaban, J., Zimmerman-Bier, B. & Wagner, G. C. Autism spectrum disorders: concurrent clinical disorders. *J Child Neurol* **23**, 6-13 (2008). https://doi.org:10.1177/0883073807307102
74 Hastings, M. H., Maywood, E. S. & Brancaccio, M. Generation of circadian rhythms in the suprachiasmatic nucleus. *Nat Rev Neurosci* **19**, 453-469 (2018). https://doi.org:10.1038/s41583-018-0026-z
75 Hasin, Y., Seldin, M. & Lusis, A. Multi-omics approaches to disease. *Genome Biol* **18**, 83 (2017). https://doi.org:10.1186/s13059-017-1215-1
76 Subramanian, I., Verma, S., Kumar, S., Jere, A. & Anamika, K. Multi-omics Data Integration, Interpretation, and Its Application. *Bioinform Biol Insights* **14**, 1177932219899051 (2020). https://doi.org:10.1177/1177932219899051